ION CLEARING in the XLS-ring

Eva S. Bozoki and Henry Halama[*]
Brookhaven National Laboratory, Upton, NY, 11973

ABSTRACT

The mechanism of ion capture by the beam, their effects on the beam as well as ways to clear the ions are discussed. Special attention is given to these questions for the SXLS ring.

INTRODUCTION

The electron beam in a storage ring collides with the residual gas in the vacuum chamber. As a consequence, low velocity positive ions are produced and are attracted by the potential well of the electron beam [1,2]. They perform stable or unstable oscillations around the beam under the repetitive Coulomb force of the bunches [1,3]. If not cleared, the captured ions can lead to partial or total neutralization of the beam, causing both, a decrease of life-time and a change in the vertical tunes as well as an increase in the tune-spread. It can also cause coherent and incoherent transverse instabilities [4,5]. More detailed treatment of the XLS ion clearing can be found in [6].

BEAM IONIZATION and NEUTRALIZATION

Relativistic electrons ($\beta \approx 1$) ionize the residual gas with a production rate of [1,7]:

$$R_p = \frac{N}{\tau} = N\sum_i \frac{1}{\tau_i} \qquad \text{and} \qquad R_i = \frac{1}{\tau_i} = d_i \sigma_i c = \sigma_i c \frac{P_i}{R_g T}$$

where N = total number of electons in the beam, σ_i = ionization cross section in m^2, d_i = molecular density in m^{-3}, P_i = partial pressure in Torr, T = temperature in $^\circ K$, c = speed of light, R_g = ideal gas constant (1.0356 10^{-25}) and the summation is for all species of ions present.

The neutralization factor is defined as the ratio of the number of ions to the number of electrons in the ring: $\eta = d_{ions} / d_e$. The time to reach η neutralization is $t = \eta\tau$ sec, that is the ions (of mass Am_p) have to be removed after travelling a distance: $1 = V_{ion} t$.

Table-1 shows the calculated ionization cross sections (see ref.[1]), ionization times and rates at T = 300° K and with P_m partial pressures taken from [8]. The calculations were carried out for different ionic species under Phase-1 and 2 conditions (γ = 391 and 1362, respectively).

Table-1
Ionization cross section, ionization time and rate for different ions at T=300 °K with γ = 391 and 1362.

molecule	σ_i $10^{-22} m^2$	τ_i sec	R_i ion/sec	σ_i $10^{-22} m^2$	τ_i sec	R_i ion/sec
	Phase-1	(γ = 391)		Phase-2	(γ = 1362)	
H_2	0.254	3.13	0.32	0.278	2.87	0.35
CO	1.41	1.04	0.96	1.59	0.93	1.07
CO_2	2.23	4.65	0.21	2.50	4.15	0.24
total		0.67			0.61	

In the absence of magnetic field, the ions move with thermal velocities [1] of

$$V_{th} = \sqrt{\frac{3kT}{m_p}} \, \frac{1}{\sqrt{A}} \qquad [m/sec].$$

In the bending magnets, the trapped ions perform a cycloidal motion [1,3,9] due to the combined action of the longitudinal electric field of the beam and the vertical magnetic field of the dipole. The resulting longitudinal velocity, the "drift"-velocity is

$$V_D = \frac{\vec{E_z} \times \vec{B_z}}{B_z^2} \frac{\omega_L^2}{\omega_L^2 + \omega_z^2} = \frac{E_z}{B_z} \frac{\omega_L^2}{\omega_L^2 + \omega_z^2}, \quad \omega_L = \frac{eB_z}{Am_p} = k_L \frac{B_z}{A} \quad (1)$$

In eq. (1), ω_L is the Larmour frequency and ω_z^2 is the cyclotron frequency.

The V_{th} thermal ion velocities and the drift velocities together with their corresponding l_D and the l_{th} distances are given in Table-2 for different ionic species under Phase-1 and 2 conditions (B_z=1.1 and 3.85 Tesla) and assuming I = 0.5 Amp current, T = 300 °K temperature, $\eta = 10^{-3}$ neutralization and with E_z fields taken at the beam surface.

One can see, that outside the dipoles, the heavier ions can travel only ≈ 0.25 m without clearing before the neutralization will reach 10^{-3}. The higher neutralization we can tolerate, the longer this "clear-free-path" will be.

Table-2
Thermal and drift velocities and the corresponding travel-distances for different molecules under Phase-1 and 2 conditions (γ=391 and 1362, B_z=1.1 and 3.85 Tesla) assuming I = 0.5 Amp current, T = 300 °K temperature and $\eta = 10^{-3}$ neutralization.

molecule	V_{th} 10^3 m/s	V_D 10^3 m/s	l_{th} m	l_D m	V_D 10^3 m/s	l_{th} m	l_D m
		Phase-1			Phase-2		
H_2	1.93	28.9	1.29	19.4	30.2	1.16	18.1
CO	0.52	02.2	0.35	1.5	06.6	0.31	4.0
CO_2	0.41	01.4	0.37	0.9	04.5	0.25	2.7

ION CLEARING

The electric field due to uniform ρ space charge density in an elliptic beam with horizontal and vertical dimensions of

$$2a = 2\sqrt{2}\sigma_x = 2\sqrt{\epsilon_x \beta_x + (\sigma_E \eta_x)^2} \qquad \text{and} \qquad 2b = 2\sqrt{2}\sigma_y = 2\sqrt{\epsilon_y \beta_y}$$
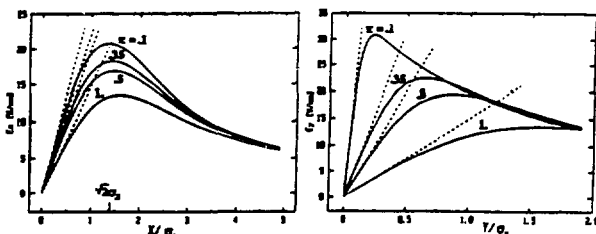
was calculated [3,10] as:

$$E_{x,y} = \frac{\rho}{\epsilon_0} \frac{1}{1 + \sigma_{x,y}/\sigma_{y,x}} [x,y] \qquad (4)$$

For a round and unbunched beam with λ line charge density (i.e. $a=b=r_o$, $\rho = \frac{\lambda}{\pi r_o^2}$), this yields:

$$E_r = \frac{\lambda}{2\pi\epsilon_0} \begin{cases} r/r_o^2 & r \leq r_0 \\ 1/r & \text{if} \quad r \geq r_o \end{cases}$$

For a bi-Gaussian charge density distribution, $E_{x,y}$ is calculated as in [11,12] using the complex error function.

E_x as a function of x (at y=0) and E_y as a function of y (at x=0) are plotted on Figs. 1 for bi-Gaussian (solid lines) and uniform (dotted lines) distribution at different values of the $\kappa = \sigma_y/\sigma_x$. All curves correspond to I=0.5 Amp.

Figs. 1
(a) E_x as a function of x along y=0 and (b) E_y as a function of y along x=0 for elliptic bi-Gaussian beam for different values of $\kappa = \sigma_y/\sigma_x$

One can see, that the electric field E of the beam increases with the distance from the beam axis inside the beam and it is the highest on the beam surface. Outside the beam, the field decreases with increasing distance.

The minimum E value for clearing of the ions is calculated from eq. (4) for uniform unbunched beam of intensity 1 Amp:

$$E^{clr} = E_x \, (x=\sqrt{2}\sigma_x) = E_y \, (y=\sqrt{2}\sigma_y) = \frac{1}{\sqrt{2}\pi c \epsilon_0 (\sigma_x + \sigma_y)}.$$

These values represent an upper limit for the minimum clearing field, since $E_{x,y}$ at the beam surface are larger for uniform then for bi-Gaussian charge distribution as can be seen from Figs. 1.

[†] The computer program CHAMP was used to evaluate eq.(5), which was obtained from CERN, curtesy of Rui Alvares-Pires and A. Poncet.

From the clearing field one can calculate the required voltage on a clearing electrode. Assuming that the clearing electrode is separated from the opposite wall of the vacuum chamber by D distance (see Fig. 2), a rough estimate is given by V [Volt] $= E^{clr}$ [Volt/m] D [m].

More realistic estimate can be obtained using the program POISSON. The calculations were performed for different geometries as shown on Fig. 2.
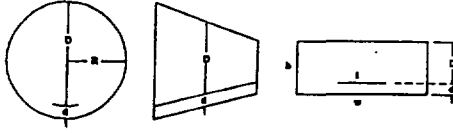

Fig. 2
Vacuum chamber with clearing electodes at different locations
in the XLS ring: (a) middle of straight section
(b) before/after Dipole (c) middle of Dipole.

The minimum clearing field, E_y^{clr} for uniform and bi-Gaussian charge density distribution as well as the necessary clearing voltage from eq. (6) and from simulations with POISSON are given in Table-3. All calculations were performed for I=0.5 Amp, ζ=.1 coupling, vacuum chamber and clearing electrode geometry as shown on Fig. 2, and beam sizes as shown on Fig. 4. (Details of the POISSON simulation including the dependence of the clearing voltages on the l and d width, D separation and ζ coupling are given in the Appendix of [6]).

Table-3
Clearing field and voltage for uniform and bi-Gaussian charge
density distribution assuming I=0.5 Amp.

location	E_y^{clr} [V/mm]		V^{clr} [kV] uniform	
	uniform	bi-Gaussian	eq.(6)	POISSON
middle of straight	20.5	15.8	1.6	1.7
before/after Dipole	25.0	18.0	1.4	1.5
middle of Dipole	34.5	21.7	1.3	1.4

As can be seen from Fig. 1, E_y^{clr} depends on the horizontal- vertical coupling, ζ. The beam sizes on Fig. 4, thus the calculations in Table-4, correspond to $\zeta = 0.1$. To illustrate how the necessary clearing field might change for different coupling, $E_y^{\zeta}/E_y^{\zeta=.1}$ is plotted as a function of ζ on Fig. 3 (for uniform distribution).
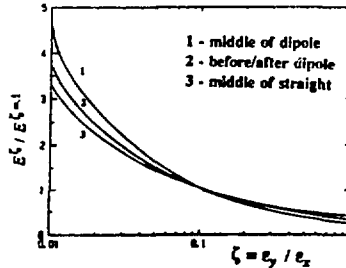

Fig. 3
Minimum clearing field as a function
of the horizontal-vertical coupling.

POTENTIAL WELLS

The $V = -\int E ds$ potential in a round vacuum chamber of radius R_o with the boundary condition $V = 0$ at $r = R_o$ is:

$$V = \frac{\lambda}{2\pi\varepsilon_o} \begin{cases} \dfrac{r^2}{2r_o^2} - \dfrac{1}{2} - \ln\dfrac{R_o}{r_o} & \text{if } r \leq r_o \\ \\ \ln\dfrac{r}{r_o} & \text{if } r \geq r_o \end{cases}$$

The potential of an elliptic beam displaced by Δx in a round vacuum chamber is given in [13]. The potential of an elliptic beam in in an elliptic (rectangular) vacuum chamber of 2w and 2h width and height, was calculated in [14]. For Gaussian charge distribution the potential was calculated in [11,15].

In case of uniform, unbunched beam, the ions are trapped if their trans-

verse energy is less than $E = eV$ [joule]. In a field-free section of the ring the ions will drift towards the deepest potential well resulting from changing vacuum chamber or beam size.

Figs. 4a and b show the (w,h) half width and height of the vacuum chamber, the $\sigma_{x,y}$ half beam size and the calculated beam potential on the beam surface for 1/4 of the
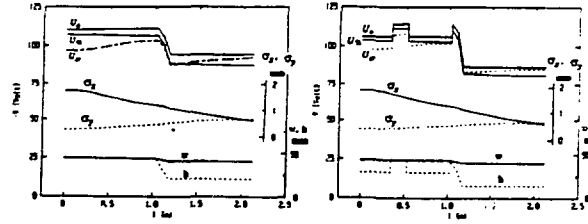

Fig. 4
Beam potential (a) for unobstructed vacuum chamber and
(b) in the presence of strip-lines.

XLS ring. The calculations were performed assuming I=0.5 Amp beam current. U_o, U_t, U_t, U_- and U_- denotes the potential in the middle of the beam and at the upper, lower, right and left surface of the beam. In case of Fig.6, the vacuum chamber dimensions are modified by the presence of striplines in the straight sections and clearing electrodes in the dipole.

One can see that in the unobstructed chamber, the deepest potential well are before entering the dipoles. There are also shallow wells at the middle of the dipoles and at the middle of the straight sections. The presence of the striplines introduces a potential well of depth equal to that of the one before the dipole, but it is less bothersome since the striplines can also be used as clearing electrodes if necessary.

CRITICAL MASS

The longitudinal velocity of ions is negligible compared with that of the electron beam, the ions are "kicked" by the electron bunches and they drift freely between the kicks. Ions, heavier than a critical mass, A_c will be trapped. This effect of kick and drift can be described in the usual matrix formalism, which yields

$$A_c = \frac{C^2 r_p I}{2ecn_B^2} \frac{1}{\sigma_y (\sigma_x + \sigma_y)}$$

where r_p is the classical proton radius and I is the beam current. With I=0.5 Amp in 6, 3 or 1 bunches, A_c was calculated to be $A_c \leq .026$, 0.11 and 0.95, respectively. That is, all ions are trapped under usual conditions in the XLS ring. The critical current, under which an ion of atomic number A is trapped is given in Table-4 for A=2, 28 and 44 and at three locations in the ring. (I=0.5 Amp and n_B=1 was assumed).

Table-4
Critical current assuming I=0.5 Amp, n_B=1.

location	I_c [Amp]		
	A=2	A=28	A=44
middle of straight	1.1	14.7	23.1
end of Dipole	1.4	19.4	30.6
middle of Dipole	1.4	19.3	30.3

Another way to help to remove ions is to shake the beam with an RF frequency which is close to both, the beam's betatron frequency and the ion bounce frequency [16,17], especially near the ion pockets. Shaking is most efficient, when combined with the use of clearing electrodes [18,19].

TUNE SHIFT

The tune shift, caused by the ions is:

$$\Delta v_{x,y} = \frac{1}{4\pi} \int \beta_{x,y}(s) k_{x,y}(s) ds, \quad where \quad k_{x,y} = \frac{e}{\gamma m_e c^2} \frac{\partial E}{\partial[x,y]}$$

and E is calculated from eq. (4) using the

$$\rho = \rho_{ion} = \frac{eN\eta}{C} \frac{1}{2\pi\sigma_x\sigma_y}$$

ion charge density. Averaging instead of integration and substituting $<\beta> = R/\nu_{x,y}$, one gets:

$$\Delta\nu_{x,y} = r_e \frac{1}{\gamma} \frac{R}{\nu_{x,y}} \frac{\eta N}{2\pi\sigma_{x,y}(\sigma_x+\sigma_y)}$$

Assuming I=0.5 Amp and $\eta=10^{-3}$, the upper limit for tune change is

$$\Delta\nu_x \le \begin{cases} .0005 \\ .0002 \end{cases} \quad \Delta\nu_y \le \begin{cases} .0022 \\ .0007 \end{cases} \text{ for } \begin{cases} \text{Phase-1} \\ \text{Phase-2} \end{cases}$$

PRESSURE BUMP

Trapped ions lower beam lifetime in the same way as residual mulecules. The pressure or density increase due to trapped ions is given by [1]:

$$\Delta P_i = \frac{\lambda}{e} \frac{1}{\pi r_o^2} \frac{1}{3.3 \ 10^{22}} \eta$$

For I=0.5 Amp, r_o=1 mm and $\eta = 5 \ 10^{-3}$, one obtains $\Delta P_i = 5 \ 10^{-10}$ Torr.

This represents more then 10 % of the total pressure and would lower the beam lifetime by the same amount. However, since heavier ions stay longer in the beam, the effect on the lifetime would be worse.

In addition to the pressure bump ΔP_i, the negative voltage applied to the clearing electrodes will accelerate electrons, produced both by the beam and by the photons, away from the clearing electrodes and towards the wall of the vacuum chamber, causing desorption of neutral molecules by electron stimulated desorption. This increase in pressure will be most significant at the beginning of commissioning due to contaminated beam tube and will decrease with beam conditioning.

CLEARING ELECTRODES

The ions will be removed by a system of clearing electrodes as shown in Fig. 5.

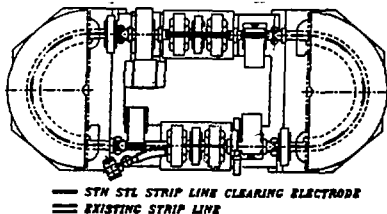**—— STN STL STRIP LINE CLEARING ELECTRODE**
═══ EXISTING STRIP LINE

Fig. 5
Location of clearing electrodes in the XLS ring.

All clearing electrodes will be terminated with lossy coax cables of the same characteristic impedance Z_o, in order to minimize machine impedance effects [20]. All dedicated clearing electrodes and their feedthrues will be rated for 5kV, well above the required $\approx$ 1.5kV (see under "Ion Clearing").

Finally, the heat induced in the electrodes by the circulated beam (see next section) must be removed by providing a thermal path to room temperature. In a cold bore machine the heat would have to be removed at liquid He temperature, which for the XLS represents a substantial heat load.

Heat flux given in Table-5 was calculated with $\rho = 9 \ 10^{-7}$ [Ohm m], I=0.5 Amp beam current, 6 and 3 bunches in the ring and $l_B = 2(2\sigma_B)$ as bunch length for Phase-1 and 2 (σ_B = 1.6 and 3.8 cm, respectively)

Table-5

n_B	charge distribution	Phase-1	Phase-2
		$<$P$>$ [Watts/m]	
6	Gauss	1.17	0.32
	cos-square	1.78	0.48
	uniform	1.07	0.30
3	Gauss	2.35	0.97
	cos-square	3.58	0.64
	uniform	2.05	0.59

CONCLUSIONS

As could be expected, the rather small circumference and bunch spacing in the XLS result in complete trapping of all residual gas ions; all ionic species are trapped since under normal working conditions the critical mass is $A_c < 1$.

The horizontal and vertical tune shifts are tolerable even for $\eta = 5 \ 10^{-3}$. The higher is the vertical value, which is $\nu_y \le .01$ and 0.002 for Phase-1 and 2, respectively.

The worst neutralization pocket ($\approx$16 %) occurs before entering the dipole, therefore one must have clearing in that region. There is a slight decrease ($\approx$2.5 % and $\approx$4 %) in the potential at the middle of the dipole and in the straight section, respectively. Abrupt changes in the vacuum chamber dimension (e.g. striplines or other "intrusions") also result in $\approx$8 % ionization pockets.

Depending on the upper limit of η that we can tolerate, clearing is needed by intervalls not much longer than the "clear free path" for the CO_2 ions. With $\eta=10^{-3}$, this is $\approx$0.25 m in the straight sections, where the ions travel with thermal velocity, and $\approx$0.9 and $\approx$2.7 m in the dipole (for Phase-1 and 2, respectively).

The necessary clearing voltages assuming 10 % horizontal-vertical coupling, I=2.5 cm wide clearing electrodes at 3.3 mm distance from the bottom of the vacuum chamber are 2.7, 2.0 and 1.4 Volt in the straight section, before and after the dipoles and at the middle of the dipole. For 1 % coupling the corresponding voltages are 8.6, 7.4 and 6.4 Volt.

A clearing rate of $\approx 10^{14}$ ion/sec is required to maintain $\eta \le 10^{-3}$.

REFERENCES

[1] Y.Baconier: Neutralization of accelerator beams by ionization of the residual gas, CERN 85-19, 1985.
[2] J.Herrera: Electron clearing for the ISA proton beam, BNL 50533,1976.
[3] R.D.Kohaupt: Ion clearing mechanism in the electron-positron storage ring Doris, DESI H1-71/2, 1971.
[4] G.Parsen: BNL 50842, 1978.
[5] E.Jones, F.Pedersen, A.Poncet, S. van der Meer, E.J.N.Wilson: Transverse instabilities due to beam-trapped ions and charged matter in the CERN Antiproton Accumulator, CERN/PS85-15 (AA)
[6] E. Bozoki, H.Halama: Ion related problems for the SXLS-ring, Submitted to Particle Accelerators.
[7] M.S.Zisman, S.Chattopadhyay, J.J.Bisogano: ZAP user's manual, LBL-21270 UC-28, 1986.
[8] H.Halama: Summary of X-ray ring performance before the 1987 shutdown, BNL-39768, 1987.
[9] R.C.Gluckstern, A.G.Ruggiero: Ion production and trapping in electron rings, BNL-26585, 1979.
[10] Y.Baconier, G.Brianti: The stability of ions in bunched beam machines, CERN/SPS/80-2 (DI), 1982.
[11] M.Basetti, G.A.Erskine: Closed expression for the electrical field of a two-dimensional Gaussian charge, CERN-ISR-TH/80-06, 1980.
[12] J.C.Godot, K.Hubner, A.Poncet: Comparison of the electric field in the beam to the available clearing fields in EPA, Note-PS/LPI/87-25.
[13] J.Herrera, B.Zotter: Average neutralization and transverse stability in Isabelle, BNL 50980, 1978.
[14] G.Grobner, K.Hubner: Computation of the electrostatic beam potential in vacuum chamber of rectangular cross-section, CERN/ISR-TH-VA/75-27, 1975.
[15] R.Alves Pires: Conformal mapping for two dimensional electrostatic beam potential calculations, CERN-PS/87-66 (AA).
[16] R.Alves Pires, D.Mohl, Y.Orlov, F.Pedersen, A.Poncet, S. van der Meer: On the Theory ofcoherent instabilities, CERN/PS/89-14 (AR)
[17] T.Kasuga, H.Yonehara, T.Kinoshita, M.Hasumoto: Japanese Journal of Applied Physics, 24,9,1985.
[18] A.Poncet, Y.Orlov: Ion shaking tests, PS/ML/Note 89-1.
[19] T.Kasuga: Ion-clearing system of UVSOR storage ring, Japanese Journal of Applied Physics, 25,11,1986.
[20] J. Wang, unpublished.

DISCLAIMER